HAL
open science

Frustration on a centered pyrochlore lattice in metal-organic frameworks

Rajah Nutakki, Richard Röss-Ohlenroth, Dirk Volkmer, Anton Jesche, Hans-Albrecht Krug von Nidda, Alexander A. Tsirlin, Philipp Gegenwart, Lode Pollet, L.D.C. Jaubert

To cite this version:

Rajah Nutakki, Richard Röss-Ohlenroth, Dirk Volkmer, Anton Jesche, Hans-Albrecht Krug von Nidda, et al.. Frustration on a centered pyrochlore lattice in metal-organic frameworks. Physical Review Research, 2023, 5, pp.L022018. 10.1103/PhysRevResearch.5.L022018 . hal-03617124v2

HAL Id: hal-03617124

https://hal.science/hal-03617124v2

Submitted on 24 Apr 2023

HAL is a multi-disciplinary open access archive for the deposit and dissemination of scientific research documents, whether they are published or not. The documents may come from teaching and research institutions in France or abroad, or from public or private research centers.

L'archive ouverte pluridisciplinaire **HAL**, est destinée au dépôt et à la diffusion de documents scientifiques de niveau recherche, publiés ou non, émanant des établissements d'enseignement et de recherche français ou étrangers, des laboratoires publics ou privés.

Frustration on a centred pyrochlore lattice in metal-organic frameworks

Rajah Nutakki,[1,2] Richard Röß-Ohlenroth,[3] Dirk Volkmer,[3] Anton Jesche,[4] Hans-Albrecht Krug von Nidda,[5] Alexander A. Tsirlin,[4] Philipp Gegenwart,[4] Lode Pollet,[1,2] and Ludovic D. C. Jaubert[6]

[1] *Arnold Sommerfeld Center for Theoretical Physics, University of Munich, Theresienstr. 37, 80333 München, Germany*
[2] *Munich Center for Quantum Science and Technology (MCQST), Schellingstr. 4, 80799 München, Germany*
[3] *Chair of Solid State and Materials Chemistry, Institute of Physics, University of Augsburg, D-86159 Augsburg, Germany*
[4] *Experimental Physics VI, Center for Electronic Correlations and Magnetism, Institute of Physics, University of Augsburg, 86159 Augsburg, Germany*
[5] *Experimental Physics V, Center for Electronic Correlations and Magnetism, Institute of Physics, University of Augsburg, 86159 Augsburg, Germany*
[6] *CNRS, Université de Bordeaux, LOMA, UMR 5798, 33400 Talence, France*

(Dated: January 31, 2023)

Geometric frustration inhibits magnetic systems from ordering, opening a window to unconventional phases of matter. The paradigmatic frustrated lattice in three dimensions to host a spin liquid is the pyrochlore, although there remain few experimental compounds thought to realize such a state. Here we go beyond the pyrochlore via molecular design in the metal-azolate framework [Mn(II)(ta)$_2$], which realizes a closely related centred pyrochlore lattice of Mn-spins with $S = 5/2$. Despite a Curie-Weiss temperature of -21 K indicating the energy scale of magnetic interactions, [Mn(II)(ta)$_2$] orders at only 430 mK, putting it firmly in the category of highly frustrated magnets. Comparing magnetization and specific heat measurements to numerical results for a minimal Heisenberg model, we predict that this material displays distinct features of a classical spin liquid with a structure factor reflecting Coulomb physics in the presence of charges.

Over the last few decades, the theoretical study of magnetism on geometrically frustrated lattices has proven highly successful in identifying exotic states of matter, ranging from classical spin ice [1, 2] to quantum spin liquids [3–5]. In 3 dimensions, the most well-studied frustrated lattice is arguably the pyrochlore lattice of corner-sharing tetrahedra. For the classical nearest neighbor Ising and Heisenberg models on the pyrochlore lattice, the spin liquid ground states have an elegant description in terms of an emergent $U(1)$ gauge field which leads to their characterization as Coulomb spin liquids [6, 7], with excitations interacting via an effective Coulomb potential and characteristic pinch point singularities in the spin structure factor. The clearest experimental realization is found in the spin ice compounds $Dy_2Ti_2O_7$ and $Ho_2Ti_2O_7$ [8], where the local orientations of the spins and dipolar interactions introduce additional energetic (rather than purely entropic) Coulomb interactions, which in turn leads to a description of excitations in terms of magnetic monopoles [9]. In the Heisenberg case, recent experiments on the transition metal pyrochlore fluoride, $NaCaNi_2F_7$, find that it is well described by an $S = 1$ pyrochlore Heisenberg antiferromagnet (PHAF) and thought to realize a Coulomb-like phase [10]. Unfortunately, it is a recurrent theme for Heisenberg materials that further neighbor interactions, anisotropic exchanges or disorder perturbs the spin-liquid physics at low temperatures [2, 11–14].

Recently, metal-organic frameworks have emerged as a class of materials for realizing strongly magnetically frustrated systems [15], offering a new avenue to realizing both familiar and novel geometrically frustrated lattices in the lab. Here, our focus is on the metal-azolate frameworks [M(II)(ta)$_2$], where M(II) is a divalent metal ion and H-ta = 1H-1,2,3-triazole, which exhibit a diamond net with vertices made of M-centred (MM$_4$) tetrahedra [Fig. 1], offering the exciting possibility to engineer novel magnetic structures by inserting additional, magnetically active ions into the pyrochlore lattice. However, so far only a handful of works have addressed their magnetic properties [16–21].

In this Letter, we explore the potential of metal-azolate frameworks in the context of frustrated magnetism by studying [Mn(ta)$_2$], which realizes a centred pyrochlore lattice. Using a combination of specific-heat and magnetic measurements, ab-initio calculations, Monte Carlo simulations, exact diagonalization and analytical insights, we predict the existence of a finite temperature regime around $T \approx 2$ K where we expect to find the hallmarks of an underlying classical spin liquid in the *minimal* model. The correlations in this spin liquid can be understood in the Coulomb framework as a dense fluid of charges created by the center spins, reminiscent of the monopole fluid studied in the context of spin ice [22, 23].

Minimal model – Adapting the synthesis procedure of Ref. [24], [Mn(ta)$_2$] was prepared as a white powder sample. Rietveld refinements of X-ray diffraction data find that [Mn(ta)$_2$] has the cubic symmetry of the $Fd\bar{3}m$ space group [17] which we confirm through high-resolution X-ray

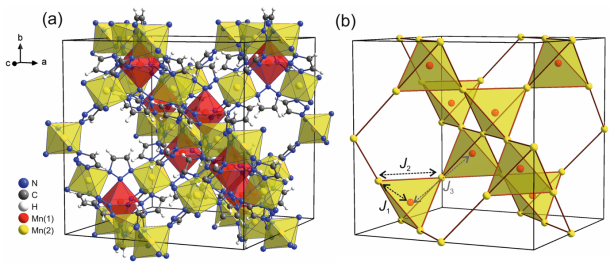

FIG. 1. **a,** Combined ball-and-stick and polyhedra model of cubic [Mn(II)(ta)$_2$] highlighting the positions of divalent octahedrally coordinated Mn ions arranged in a diamond-type lattice (CSD code: HEJQEV). The metal centres differ with respect to their special crystallographic positions and coordination environments: Mn(1) is located on Wyckoff position 8b (site symmetry $\bar{4}3m$), coordinated exclusively by the N2 donor atoms of the μ_3-bridging triazolate linker; Mn(2) is found at Wyckoff position 16d (site symmetry $\bar{3}m$), coordinated exclusively by N1 or N3 donor atoms. **b,** Schematic representation of the centred pyrochlore lattice with magnetic exchange paths for first (J_1, Mn(1)−Mn(2), 3.929Å), second (J_2, Mn(2)−Mn(2), 6.416Å) and third (J_3, Mn(1)−Mn(1), 7.858Å) neighbors. Mn(1) and Mn(2) are respectively labeled centre (orange) and corner (yellow) spins.

powder diffraction at 5 K. Since the 3d valence band of high-spin Mn(II) ions is half filled, we expect its magnetic moment to be isotropic. Previous conductivity measurements together with periodic DFT band structure calculations [25] classified this compound as a wide-bandgap semiconductor with a bandgap $\Delta = 3.1$ eV $\equiv 36\,000$ K. We therefore consider [Mn(ta)$_2$] an insulator at temperatures $T \ll \Delta$. To assess the relevance of different exchange pathways [Fig. 1], we performed DFT calculations assuming isotropic exchanges for high-spin 3d^5 Mn(II) ions between first (J_1), second (J_2) and third (J_3) neighbors [see Fig. 1.b and Supplementary Information [26]]. We obtain that $J_1^{\rm DFT} \sim 2-4$ K and $\gamma^{\rm DFT} \equiv J_1^{\rm DFT}/J_2^{\rm DFT} \approx 1.3-1.65$. The fact that $J_1^{\rm DFT}$ and $J_2^{\rm DFT}$ are of the same order of magnitude is likely due to the similar exchange pathways, traversing either two or three nitrogen ions respectively along the triazolate ligand. On the other hand, no such pathway is available beyond second neighbors, hence $|J_3^{\rm DFT}| < 0.01$ K $\ll J_1^{\rm DFT}, J_2^{\rm DFT}$. Thanks to this separation of scales, it suffices to define a minimal model (CPy) on the centred pyrochlore lattice with only first and second neighbor isotropic couplings,

$$H = J_1 \sum_{\langle ij \rangle} \mathbf{S}_i \cdot \mathbf{S}_j + J_2 \sum_{\langle\langle ij \rangle\rangle} \mathbf{S}_i \cdot \mathbf{S}_j - \mu_0 \mathbf{H} \cdot \sum_i \mathbf{S}_i. \quad (1)$$

Confirming that [Mn(ta)$_2$] is described by Hamiltonian (1), requires the appropriate theoretical tools. Fortunately, owing to the large magnetic moment $S = 5/2$ we can resort to classical Monte Carlo simulations, which have proven to be powerful techniques to describe magnetic properties of pyrochlore materials capable of capturing long-range order as well as unconventional correlations of spin liquids [2, 27–31]. Continuous-spin models cannot, however, reproduce specific heat at very low temperatures because entropy is ill defined. There, one needs to consider the discrete nature of quantum spins via *e.g.* exact diagonalization (ED). Since ED for $S = 5/2$ is particularly costly in computer time and memory, we will restrict calculations to a single tetrahdral unit of five spins, fitted to high-temperature experimental data. Such an approximation shall provide an independent estimate of the energy scales, to be compared with parameters obtained from DFT and Monte Carlo simulations. In the rest of this paper, $\mathbf{S}_i$ will denote a 3-component classical spin of length $|\mathbf{S}_i| = 5/2$, except when analyzing specific-heat data where $\mathbf{S}_i$ is a quantum $S = 5/2$ spin.

Comparison between experiment and theory − To explore the magnetism of [Mn(ta)$_2$], we measured magnetic susceptibility over three decades in temperature. Fitting the high-temperature regime ($T > 200$ K) of the susceptibility χ with a Curie-Weiss law [Fig. 2.a], we obtain an effective magnetic moment $\mu_{\rm eff} = 6.05\ \mu_B$ per Mn ion and a Curie-Weiss temperature $\Theta_{CW} = -21$ K. These values agree with a previous report [17] (5.8 μ_B and −21.9 K respectively) and with the expected size of the magnetic moment $g_S\sqrt{S(S+1)} = 5.9\ \mu_B$ which is a stable value for a Mn(II) ion with high-spin 3d^5 electronic configuration. Θ_{CW} indicates sizeable antiferromagnetic interactions. However, our specific heat measurements do not find a transition until a low $T_c = 0.43$ K [Fig. 2.c]. For comparison, the degree of frustration $f \equiv \frac{|\Theta_{CW}|}{T_c} = 49$ is of the same order as the one of the celebrated Kitaev materials [13, 32] and substantially larger than the one of most rare-earth pyrochlore oxides [2, 11, 12]. It means that not only does [Mn(ta)$_2$] offer an unexplored geometry, but one can also expect a sizeable temperature range above T_c where frustration is important.

Our main result is the agreement between experiments and Monte Carlo simulations for the (i) magnetic susceptibility in Fig. 2.a, and (ii) magnetization curves in Fig. 2.b, using coupling parameters that confirm the DFT estimates, $J_1^{\rm MC} = 2.0$ K and $\gamma^{\rm MC} = 1.51 \pm 0.15$. Further support for this claim is seen in the fit of the specific heat [Fig. 2.c]: The bump at ~ 4 K is also consistent with finite-temperature exact diagonalization for $J_1^{\rm ED} = 1.95$ K and $\gamma^{\rm ED} \sim 1.75$ [Fig. 2.c]. While the value of $\gamma^{\rm ED}$ should only be considered as a qualitative estimate, the ED results indicate that the bump at 4 K corresponds to a growth of the

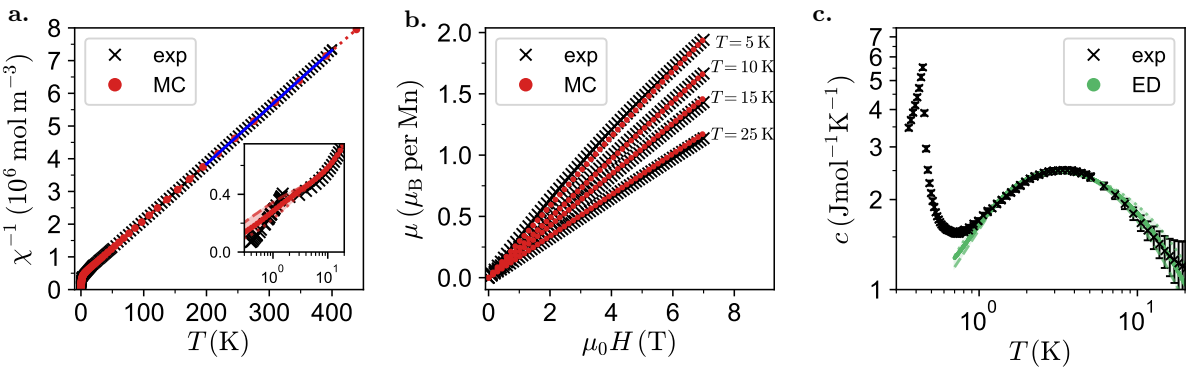

FIG. 2. **Comparison between experiment and theory for [Mn(ta)$_2$].** **a.** Curie-Weiss fit (blue, for $T > 200$ K) of the inverse susceptibility χ^{-1} obtained from magnetization measurements $\chi = M/H$ (black) and MC simulations of over 41000 spins (red). Inset, the inverse susceptibilities at low temperatures. The Curie-Weiss fit yields a Landé factor of $g = 2.05$. **b.** Magnetization in an external field over a broad temperature range. MC simulations compare well to experimental magnetization measurements at $T > 1$ K for $J_1^{\mathrm{MC}} = 2.0$ K, $\gamma^{\mathrm{MC}} = 1.51 \pm 0.15$. **c.** The specific heat of [Mn(ta)$_2$] displays a broad bump at ~ 4 K and a sharp peak at 0.43 K. The former is qualitatively reproduced by full diagonalization for $J_1^{\mathrm{ED}} = 1.95$ K and $\gamma^{\mathrm{ED}} \sim 1.75$ up to a rescaling by a factor of 0.8 along the $y-$axis. In order to show the γ dependence of Hamiltonian (1), simulation curves in **a.** and **c.** are supplemented by dotted and dashed lines corresponding to $\pm 10\%$ variations of γ.

correlation length beyond a single frustrated unit. The region $0.43 < T \lesssim 4$ K thus appears appropriate to support a potentially exotic magnetic structure, where frustrated correlations exist, but have not yet been destroyed by long-range order. We study the nature of this regime in the following.

The Centred Pyrochlore Spin Liquid – To show how the CPy model can host a spin liquid, it is convenient to rewrite Hamiltonian (1) as a sum over (centred) tetrahedra, with index α,

$$H = \frac{J_2}{2} \sum_{\alpha} |\mathbf{L}_\alpha|^2 + \text{const}, \tag{2}$$

$$\text{with } \mathbf{L}_\alpha = \gamma \mathbf{S}_{\alpha,c} + \sum_{m=1}^{4} \mathbf{S}_{\alpha,m}, \tag{3}$$

where c labels the centre spin while the sum over m runs over the four corner spins. The ground state manifold is therefore defined by minimizing $L_\alpha = |\mathbf{L}_\alpha|$ on all units. For $\gamma \geq 4$, this yields a long-range ordered ferrimagnet with 1/3 saturated magnetization where $\mathbf{S}_{\alpha,i=1,..,4} = -\mathbf{S}_{\alpha,c}$. On the other hand, for $\gamma < 4$, the ground state is defined by the local constraint

$$\mathbf{L}_\alpha = 0, \ \forall \alpha. \tag{4}$$

Such an energetic constraint, familiar from the kagome and pyrochlore lattices, is often used to define a classical spin liquid, provided order by disorder does not select an ordered state. A Maxwellian counting argument [33] gives the degrees of freedom D_n of these spin liquids. For the kagome, $D_3 = 0$ (which is famously marginally disordered), whereas $D_4 = N_u$ for the pyrochlore [33], where N_u is the number of units making up the lattice. In the CPy model, we find $D_5 = 3\,N_u$ for $\gamma \sim 1$. Similarly, these spin liquids manifest themselves via a number of flat bands F_n as the ground state of their excitation spectrum [34]: $F_3 = 1$ out of 3 bands for kagome, $F_4 = 2$ out of 4 for pyrochlore, whereas $F_5 = 4$ flat bands out of 6 for $\gamma < 4$ in the CPy model. Therefore, the CPy model hints at a notably strong spin liquid, even more disordered than the extensively studied ones on kagome and pyrochlore. This is supported by our Monte Carlo simulations [35] showing that CPy lies in the middle of a disordered ground state (found for any $\gamma \lesssim 3$) which indicates that the ordering mechanism in [Mn(ta)$_2$] lies beyond our minimal CPy model. This is often the case in frustrated magnetism [2, 11–13], where perturbations ultimately lift the ground-state degeneracy in materials. In this case, the largest perturbation is likely dipolar interactions with a nearest neighbour strength of 270 mK. Adding these to the CPy model, we find ordering at 250mK in MC simulations, where the ordered state is an unsaturated ferrimagnet and corner spins realizing a planar antiferromagnet on each tetrahedron with the remaining spin weight. Further details are provided in the supplementary information. Our simulations show that the addition of dipolar interactions does not significantly modify the properties of the model in the regime $1 < T < 4$ K, where we expect the spin liquid to persist.

An emergent charge fluid – To better understand the nature of this spin liquid and its relation to known pyrochlore physics we look at the magnetic correlations, best visualised through the structure factor in reciprocal space, $\mathcal{S}(\mathbf{q})$, which we obtained from our MC simulations [Figs. 3.a,b].

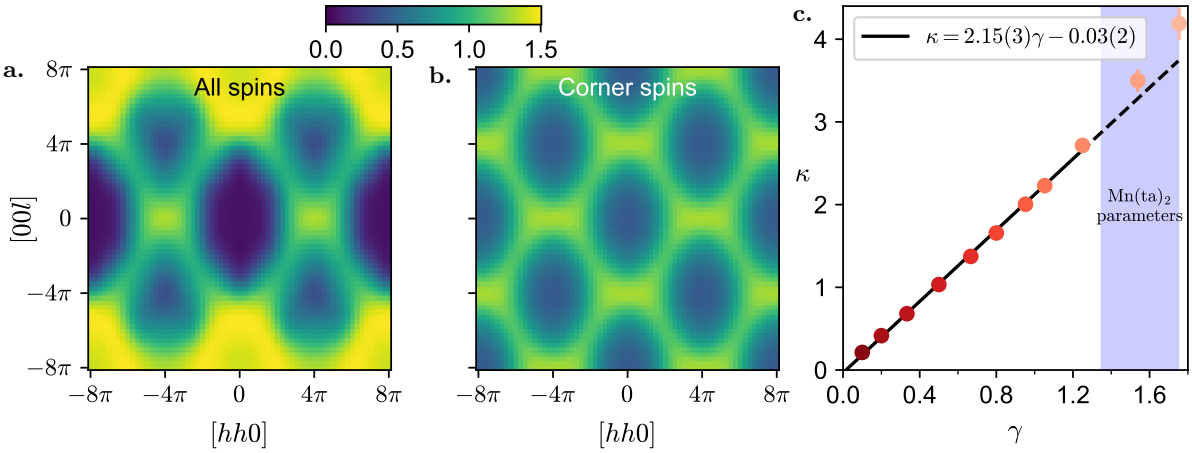

FIG. 3. Spin structure factor from large-scale MC simulations at $T = 1.5\,\mathrm{K}, \gamma = 1.5$ in the $[hhl]$ plane including all spins (**a.**) and only sites residing at the corners of tetrahedra (**b.**). Finite width bow ties at $\mathbf{q} = (\pm 4\pi, \pm 4\pi, 0)$ are found in both and the structure factor in (**b.**). is within 1% of that found at $T = 0.07\,\mathrm{K}$. **c.** The width of the bow ties in the structure factor of the effective field parametrized by κ, see Eq. 6, for different values of the coupling ratio γ at $T = 0.07\,\mathrm{K}$. A linear fit was performed to the data up to $\gamma = 1.25$ (black line).

We find that, in the regime $0 < \gamma < 2$, $\mathcal{S}(\mathbf{q})$ is characterized by finite width bow ties, which are found to arise from the correlations between spins residing at the vertices of the tetrahedra. The magnetic structure evolves continuously in this regime, with the width of the bow ties increasing with γ. This suggests that these correlations can be understood in the framework of the Coulomb phase on the pyrochlore lattice. Rewriting the constraint, Eq. (4), for each of the spin components $a \in \{x, y, z\}$ as

$$\sum_{m=1}^{4} S^a_{\alpha,m} = -\gamma S^a_{\alpha,c} = \rho^a_\alpha \tag{5}$$

we interpret ρ^a_α as a pseudoscalar ("magnetic") charge, with a strength parameterized by γ. Hence, the Coulomb description is that of an effective field coupled to charges on the diamond lattice that break the zero-divergence constraint. For small γ, the charge concentration is low, so Debye-Hueckel theory [36, 37] can be used to understand the spin correlations. In this regime, there will be entropic screening of the effective field, resulting in a Lorentzian form for its structure factor

$$\mathcal{B}^a_{aa}(q_a, q_b = 0, q_c = 0) \propto \frac{1}{q_a^2 + \kappa^2}, \tag{6}$$

where $a, b, c \in \{x, y, z\}$ and Debye-Hueckel theory predicts that $\kappa \propto \gamma$. At some value of γ, the charge concentration becomes large and we will need to account for additional corrections. Remarkably, we find that the prediction from Debye-Hueckel theory holds in MC simulations up to $\gamma \approx 1.25$, see Figs. 3.c. Thus, the correct description for the regime relevant to [Mn(ta)$_2$], $\gamma^{\mathrm{MC}} \approx 1.5$, is that of a moderately dense charge fluid, which is the Heisenberg model variant of a monopole fluid in spin ice. Whilst such a description accounts for the entropic selection of specific spin configurations, it does not account for energetic considerations necessary for a full effective description of the structure factor, such as which charge distributions enter the ground state.

Outlook – The CPy model, established as a minimal model for [Mn(ta)$_2$], displays a number of attractive features such as large, isotropic Heisenberg interactions, an unusually large number of magnetically disordered degrees of freedom (in fact, higher than for most known spin liquids), a reasonably large Ramirez frustration ratio, and a structure factor reflecting Coulomb physics in the presence of charges controlled through γ. Experimentally, external pressure may be a viable tool for controlling γ, similar to spin-1/2 frustrated magnets [38, 39]. The consequences of this picture for the inelastic spectrum and the nature of excitations are interesting open questions. Inspired by routes taken for the pyrochlores [12, 28, 40], ways to build a multitude of exotic phases by taking a selection of degrees of freedom out of the ground state, *e.g.*, via chemical substitution or with magnetic field, can be thought of. Even more broadly, [Mn(ta)$_2$] belongs to a family of metal-azolate frameworks, whose potential for low energy physics remained till recently to a large extent uncharted. These frameworks provide a versatile platform to engineer (quantum) frustrated magnetism on the centred pyrochlore lattice and beyond, such as [Fe(ta)$_2$(BF$_4$)$_x$] with a degree of frustration $f \approx 27$ [19], [Cu(ta)$_2$] with Cu(II) dimers at low temperature [18], and

[Cr(II/III)(ta)$_2$(CF$_3$SO$_3$)$_{0.33}$] with large exchange couplings [21]. While ligand substitution in similar 1,2,3-triazolate-based Mn(II) networks is known to influence their magnetic properties [41], guest molecule loading in the framework pores should further potentiate the adjustment possibilities in such materials. Thus, they offer us a near infinite playground for design and experimental characterization.

Acknowledgments – We are grateful to Nic Shannon for stimulating discussions. D.V. and R.R.-O. are grateful for financial support from DFG grant VO-829/12-2 (DFG Priority Program 1928 "Coordination Networks: Building Blocks for Functional Systems") and SEM micrographs taken by Ralph Freund. A.A.T., A.J., P.G., and H.-A. K.v.N. were supported by the German Research Foundation via TRR80. L.D.C.J. acknowledges financial support from the "Agence Nationale de la Recherche" under Grant No.ANR-18-CE30-0011-01. R.N., L.P. and L.D.C.J. acknowledge financial support from the LMU-Bordeaux Research Cooperation Program. R. N. and L. P. acknowledge support from FP7/ERC Consolidator Grant QSIMCORR, No. 771891, and the Deutsche Forschungsgemeinschaft (DFG, German Research Foundation) under Germany's Excellence Strategy – EXC-2111 – 390814868. Our simulations make use of the ALPSCore library [42].

[1] C. Castelnovo, R. Moessner, and S. Sondhi, Annual Review of Condensed Matter Physics **3**, 35 (2012).
[2] L. D. C. Jaubert and M. Udagawa, eds., *Spin Ice*, Springer Series in Solid-State Sciences, Vol. 197 (Springer, 2021).
[3] L. Savary and L. Balents, Reports on Progress in Physics **80**, 016502 (2017), arXiv:1601.03742.
[4] Y. Zhou, K. Kanoda, and T.-K. Ng, Reviews of Modern Physics **89**, 025003 (2017).
[5] J. Knolle and R. Moessner, Annual Review of Condensed Matter Physics **10**, 451 (2019).
[6] S. V. Isakov, K. Gregor, R. Moessner, and S. L. Sondhi, Physical Review Letters **93**, 167204 (2004).
[7] C. L. Henley, Annual Review of Condensed Matter Physics **1**, 179 (2010).
[8] S. T. Bramwell and M. J. Harris, Journal of Physics: Condensed Matter **32**, 374010 (2020).
[9] C. Castelnovo, R. Moessner, and S. L. Sondhi, Nature **451**, 42 (2008).
[10] K. W. Plumb, H. J. Changlani, A. Scheie, S. Zhang, J. W. Krizan, J. A. Rodriguez-Rivera, Y. Qiu, B. Winn, R. J. Cava, and C. L. Broholm, Nature Physics **15**, 54 (2019).
[11] A. M. Hallas, J. Gaudet, and B. D. Gaulin, Annual Review of Condensed Matter Physics **9**, 105 (2018).
[12] J. G. Rau and M. J. Gingras, Annual Review of Condensed Matter Physics **10**, 357 (2019).
[13] S. Trebst and C. Hickey, Physics Reports **950**, 1 (2022).
[14] E. Kermarrec, R. Kumar, G. Bernard, R. Hénaff, P. Mendels, F. Bert, P. L. Paulose, B. K. Hazra, and B. Koteswararao, Phys. Rev. Lett. **127**, 157202 (2021).
[15] J. M. Bulled, J. A. M. Paddison, A. Wildes, E. Lhotel, S. J. Cassidy, B. Pato-Doldán, L. C. Gómez-Aguirre, P. J. Saines, and A. L. Goodwin, Physical Review Letters **128**, 177201 (2022).
[16] X.-H. Zhou, Y.-H. Peng, X.-D. Du, J.-L. Zuo, and X.-Z. You, CrystEngComm **11**, 1964 (2009).
[17] F. Gándara, F. J. Uribe-Romo, D. K. Britt, H. Furukawa, L. Lei, R. Cheng, X. Duan, M. O'Keeffe, and O. M. Yaghi, Chemistry - A European Journal **18**, 10595 (2012).
[18] M. Grzywa, D. Denysenko, J. Hanss, E.-W. Scheidt, W. Scherer, M. Weil, and D. Volkmer, Dalton Transactions **41**, 4239 (2012).
[19] J. G. Park, M. L. Aubrey, J. Oktawiec, K. Chakarawet, L. E. Darago, F. Grandjean, G. J. Long, and J. R. Long, Journal of the American Chemical Society **140**, 8526 (2018), publisher: American Chemical Society.
[20] M. Grzywa, R. Röß-Ohlenroth, C. Muschielok, H. Oberhofer, A. Błachowski, J. Żukrowski, D. Vieweg, H.-A. K. von Nidda, and D. Volkmer, Inorganic Chemistry **59**, 10501 (2020).
[21] J. G. Park, Nature Chemistry **13**, 11 (2021).
[22] R. A. Borzi, D. Slobinsky, and S. A. Grigera, Physical Review Letters **111**, 147204 (2013).
[23] D. Slobinsky, G. Baglietto, and R. A. Borzi, Physical Review B **97**, 174422 (2018).
[24] C.-T. He, Z.-M. Ye, Y.-T. Xu, D.-D. Zhou, H.-L. Zhou, D. Chen, J.-P. Zhang, and X.-M. Chen, Chem. Sci. **8**, 7560 (2017).
[25] L. Sun, C. H. Hendon, S. S. Park, Y. Tulchinsky, R. Wan, F. Wang, A. Walsh, and M. Dincă, Chemical Science **8**, 4450 (2017).
[26] see the supplemental.
[27] B. Javanparast, Z. Hao, M. Enjalran, and M. J. P. Gingras, Phys. Rev. Lett. **114**, 130601 (2015).
[28] H. Yan, O. Benton, L. D. C. Jaubert, and N. Shannon, Phys. Rev. B **95**, 094422 (2017).
[29] S. Zhang, H. J. Changlani, K. W. Plumb, O. Tchernyshyov, and R. Moessner, Physical Review Letters **122**, 167203 (2019).
[30] A. M. Samarakoon, K. Barros, Y. W. Li, M. Eisenbach, Q. Zhang, F. Ye, V. Sharma, Z. L. Dun, H. Zhou, S. A. Grigera, C. D. Batista, and D. A. Tennant, Nature Communications **11**, 892 (2020).
[31] D. R. Yahne, D. Pereira, L. D. C. Jaubert, L. D. Sanjeewa, M. Powell, J. W. Kolis, G. Xu, M. Enjalran, M. J. P. Gingras, and K. A. Ross, Phys. Rev. Lett. **127**, 277206 (2021).
[32] S. M. Winter, A. A. Tsirlin, M. Daghofer, J. v. d. Brink, Y. Singh, P. Gegenwart, and R. Valentí, Journal of Physics: Condensed Matter **29**, 493002 (2017).
[33] R. Moessner and J. T. Chalker, Physical Review B **58**, 12049 (1998).
[34] J. N. Reimers, A. J. Berlinsky, and A.-C. Shi, Physical Review B **43**, 865 (1991).
[35] R. Nutakki et al., in preparation.

[36] Y. Levin, Reports on Progress in Physics **65**, 1577 (2002).
[37] C. Castelnovo, R. Moessner, and S. L. Sondhi, Physical Review B **84**, 144435 (2011).
[38] E. Kermarrec, J. Gaudet, K. Fritsch, R. Khasanov, Z. Guguchia, C. Ritter, K. A. Ross, H. A. Dabkowska, and B. D. Gaulin, Nature Communications **8**, 14810 (2017).
[39] M. E. Zayed, C. Rüegg, J. Larrea J., A. M. Läuchli, C. Panagopoulos, S. S. Saxena, M. Ellerby, D. F. McMorrow, T. Strässle, S. Klotz, G. Hamel, R. A. Sadykov, V. Pomjakushin, M. Boehm, M. Jiménez-Ruiz, A. Schneidewind, E. Pomjakushina, M. Stingaciu, K. Conder, and H. M. Rønnow, Nature Physics **13**, 962 (2017).
[40] K. A. Ross, L. Savary, B. D. Gaulin, and L. Balents, Phys. Rev. X **1**, 021002 (2011).
[41] R. Röß-Ohlenroth, M. Hirrle, M. Kraft, A. Kalytta-Mewes, A. Jesche, H.-A. Krug von Nidda, and D. Volkmer, Zeitschrift für anorganische und allgemeine Chemie **648**, e202200153 (2022), https://onlinelibrary.wiley.com/doi/pdf/10.1002/zaac.202200153.
[42] A. Gaenko, A. Antipov, G. Carcassi, T. Chen, X. Chen, Q. Dong, L. Gamper, J. Gukelberger, R. Igarashi, S. Iskakov, M. Könz, J. LeBlanc, R. Levy, P. Ma, J. Paki, H. Shinaoka, S. Todo, M. Troyer, and E. Gull, Comput. Phys. Commun. **213**, 235 (2017).